OPEN ACCESS Freely available online

PLoS GENETICS

ARGONAUTE10 and *ARGONAUTE1* Regulate the Termination of Floral Stem Cells through Two MicroRNAs in *Arabidopsis*

Lijuan Ji[1], Xigang Liu[1], Jun Yan[2], Wenming Wang[3], Rae Eden Yumul[1,4], Yun Ju Kim[1], Thanh Theresa Dinh[1,4], Jun Liu[1], Xia Cui[5], Binglian Zheng[1], Manu Agarwal[1], Chunyan Liu[5], Xiaofeng Cao[5], Guiliang Tang[2], Xuemei Chen[1]*

1 Department of Botany and Plant Sciences, Institute of Integrative Genome Biology, University of California Riverside, Riverside, California, United States of America, **2** Gene Suppression Laboratory, Department of Plant and Soil Sciences and KTRDC, University of Kentucky, Lexington, Kentucky, United States of America, **3** Rice Institute, Sichuan Agricultural University, Chengdu, China, **4** ChemGen IGERT program, Center for Plant Cell Biology, Institute of Integrative Genome Biology, University of California Riverside, Riverside, California, United States of America, **5** State Key Laboratory of Plant Genomics and National Center for Plant Gene Research, Institute of Genetics and Developmental Biology, Chinese Academy of Sciences, Beijing, China

Abstract

Stem cells are crucial in morphogenesis in plants and animals. Much is known about the mechanisms that maintain stem cell fates or trigger their terminal differentiation. However, little is known about how developmental time impacts stem cell fates. Using *Arabidopsis* floral stem cells as a model, we show that stem cells can undergo precise temporal regulation governed by mechanisms that are distinct from, but integrated with, those that specify cell fates. We show that two microRNAs, miR172 and miR165/166, through targeting *APETALA2* and type III homeodomain-leucine zipper (HD-Zip) genes, respectively, regulate the temporal program of floral stem cells. In particular, we reveal a role of the type III HD-Zip genes, previously known to specify lateral organ polarity, in stem cell termination. Both reduction in HD-Zip expression by over-expression of miR165/166 and mis-expression of HD-Zip genes by rendering them resistant to miR165/166 lead to prolonged floral stem cell activity, indicating that the expression of HD-Zip genes needs to be precisely controlled to achieve floral stem cell termination. We also show that both the ubiquitously expressed *ARGONAUTE1* (*AGO1*) gene and its homolog *AGO10*, which exhibits highly restricted spatial expression patterns, are required to maintain the correct temporal program of floral stem cells. We provide evidence that AGO10, like AGO1, associates with miR172 and miR165/166 *in vivo* and exhibits "slicer" activity *in vitro*. Despite the common biological functions and similar biochemical activities, *AGO1* and *AGO10* exert different effects on miR165/166 *in vivo*. This work establishes a network of microRNAs and transcription factors governing the temporal program of floral stem cells and sheds light on the relationships among different *AGO* genes, which tend to exist in gene families in multicellular organisms.

Citation: Ji L, Liu X, Yan J, Wang W, Yumul RE, et al. (2011) *ARGONAUTE10* and *ARGONAUTE1* Regulate the Termination of Floral Stem Cells through Two MicroRNAs in *Arabidopsis*. PLoS Genet 7(3): e1001358. doi:10.1371/journal.pgen.1001358

Editor: Li-Jia Qu, Peking University, China

Received August 15, 2010; **Accepted** February 28, 2011; **Published** March 31, 2011

Funding: The work was supported by a grant from National Institutes of Health (GM61146) to X Chen, by grants from National Basic Research Program of China (2007CB948202) to C Liu and (2009CB941500) to X Cao, by National Natural Science Foundation of China (30828002) to X Chen and X Cao, and by Transgenic Projects Funds 2008ZX08009-001 and 2011ZX08009-001 to C Liu and 2011ZX08009-001 and 2009ZX08009-39B to X Cui. TT Dihn and RE Yumul were supported by an NSF ChemGen IGERT training grant (DGE0504249). G Tang is supported by KTRDC, KSEF (# KSTC-144-401-08-029), USDA (2006-35301-17115 and 2006-35100-17433), and NSF (MCB-0718029, Subaward no. S-00000260 and IOS-1048216). The funders had no role in study design, data collection and analysis, decision to publish, or preparation of the manuscript.

Competing Interests: The authors have declared that no competing interests exist.

* E-mail: xuemei.chen@ucr.edu

Introduction

Stem cells are key to morphogenesis in multicellular organisms and understanding the mechanisms governing their maintenance or termination is a major goal in developmental biology. In plants, small populations of pluripotent stem cells are found in meristems located at the tips of roots, shoots, or developing flowers. The stem cells in the shoot apical meristem (SAM) continuously provide new cells for organogenesis to give rise to the entire above-ground portion of the plant. The SAM generates leaf primordia during vegetative growth and, after floral transition, produces floral meristems on its flanks. *Arabidopsis* floral meristems produce four concentric whorls of floral organs of fixed numbers, namely four sepals, four petals, six stamens and two fused carpels. In contrast to the SAM, floral meristems are genetically programmed to terminate after the primordia of the female reproductive organs (carpels) are formed (reviewed in [1]). The termination of floral stem cells is temporally precisely regulated to coincide with the formation of the female reproductive organs to ensure successful reproduction of plants. This property of floral stem cells, i.e. determinacy, offers an opportunity to understand the temporal regulation of stem cell maintenance.

A key factor in stem cell maintenance in plants is the *WUSCHEL* (*WUS*) gene encoding a homeodomain transcription factor. In both the SAM and the floral meristems, *WUS* is expressed in a small group of cells named the organizing center

Author Summary

Stem cells have the capacity to self renew while producing daughter cells that undergo differentiation. While some stem cells remain as stem cells throughout the life of an organism, others are programmed to terminate within developmental contexts. It is presumed that stem cell termination is simply the differentiation of stem cells into a specific cell type(s). Using floral stem cells as a model, we show that the temporally regulated termination of floral stem cells is genetically separable from stem cell differentiation, and thus we reveal the presence of a temporal program of stem cell regulation. We show that two microRNAs, miR172 and miR165/166, and two argonaute family proteins, ARGONAUTE1 (AGO1) and AGO10, regulate the termination of floral stem cells. We establish the homeodomain-leucine zipper (DH-Zip) genes, targets of miR165/166, as crucial factors in floral stem cell termination. While AGO1 is the major miRNA effector, the molecular function of AGO10 has been elusive. Here we demonstrate that AGO10 is also a miRNA effector in that AGO10 is associated with miRNAs *in vivo* and exhibits "slicer" activity *in vitro*. Despite the similar biochemical activities, AGO1 and AGO10 promote floral stem cell termination by exerting opposite effects on miR165/166.

(OC) located underneath the stem cells [2]. The OC signals to the overlying stem cells to maintain their "stemness". In loss-of-function *wus* mutants, the stem cells in both the SAM and the floral meristems terminate precociously. For example, flowers of the null *wus-1* mutant lack a full complement of floral organs and terminate in a central stamen. *WUS* expression commences as soon as the floral meristem is formed (at stage 1; stages according to [3]). By stage 6, when the carpel primordia are formed, *WUS* expression is shut off [4], and this temporally precise repression of *WUS* expression underlies the proper termination of floral stem cells.

The temporal regulation of *WUS* expression requires at least two transcription factors with opposing activities, AGAMOUS (AG) and APETALA2 (AP2), which are best known for their roles in the specification of reproductive and perianth organ identities, respectively, in flower development (reviewed in [5]). The MADS-domain protein AG promotes floral meristem termination by repressing *WUS* expression at stage 6 [6,7]. In an *ag* null mutant, such as *ag-1*, *WUS* expression persists throughout flower development [6,7] and the floral meristems lose determinacy to result in a flowers-within-flower phenotype [8]. Flowers of the *ag-1 wus-1* double mutant resemble *wus-1* flowers, indicating that *AG* causes floral stem cell termination by repressing *WUS* expression [2]. While *AG* acts to terminate floral stem cells, *AP2*, an AP2-domain containing transcription factor gene [9] regulated by the microRNA (miRNA) miR172 [10,11], promotes stem cell maintenance. In plants that express the miR172-resistant *AP2* cDNA *AP2m3* [11] from the *AP2* promoter, flowers have numerous stamens that are continuously produced by indeterminate floral meristems [12]. *WUS* expression is prolonged in *AP2p::AP2m3* flowers, and the prolonged *WUS* expression underlies the indeterminate phenotype because *wus-1* is completely epistatic to *AP2m3* [12]. *AP2* is known to repress the transcription of *AG* in the outer two floral whorls [13]. De-repressed *AP2* in *AP2m3* plants causes a moderate reduction in *AG* mRNA levels in the center of the floral meristem and this partially underlies the stem cell termination defects of *AP2m3* flowers [12]. De-repressed *AP2* also compromises floral stem cell termination in an *AG*-independent manner, which is reflected by the stronger phenotypes of *AP2m3 ag-1* relative to *ag-1* [12].

Small RNAs of 21–24 nucleotides (nt) are sequence-specific guides in RNA silencing at the transcriptional and posttranscriptional levels in plants (reviewed in [14]). ARGONAUTE (AGO) proteins associate with small RNAs and serve as effectors in RNA silencing (reviewed in [15]). Different AGO proteins associate with, and mediate the functions of, distinct types of small RNAs. Among the ten AGO proteins in *Arabidopsis*, AGO1, 2, 4, 5, 6, 7, and 9 have been shown to bind specific sets of endogenous small RNAs [16–19]. AGO1, the founding member of the family, binds most miRNAs, trans-acting siRNAs (ta-siRNAs), and transgene siRNAs and exhibits "slicer" activity, an endonucleolytic activity that precisely cleaves target mRNAs [20]. ZWILLE (ZLL)/PINHEAD (PNH), which will be hereafter referred to as AGO10 (unless specific alleles or constructs are referred to), is the most related to AGO1 among the ten *Arabidopsis* AGO proteins [21]. While *AGO1* is ubiquitously expressed [22], *AGO10* expression is restricted to meristems, the vasculature, and adaxial sides of lateral organ primordia [23,24]. *AGO10* was initially identified as a factor required for SAM maintenance [23–25]. Null mutations in *AGO10* lead to the absence of a SAM with incomplete penetrance. Examination of several miRNA target genes at the mRNA and protein levels in *ago10* mutants implicated *AGO10* in miRNA-mediated translational repression [26,27]. However, the lack of knowledge of the small RNA binding and enzymatic properties of AGO10 has hindered the understanding of the molecular mechanisms of action of AGO10 in development and in RNA silencing, especially in relationship to AGO1.

In our previous studies, we found that four genes with potential roles in RNA metabolism, *HUA1*, *HUA2*, *HUA ENHANCER2* (*HEN2*), and *HEN4*, promote *AG* expression [28]. Loss-of-function mutations in any one gene do not sufficiently compromise *AG* expression or flower development, but double or triple mutants have reduced *AG* expression and phenotypes indicative of partial loss-of-function of *AG*. In a genetic screen in the *hua1 hua2* background and in two separate genetic screens in backgrounds compromised for *AG* expression or function, we isolated *ago10* mutations with defects in floral stem cell termination. We also establish a role of *AGO1* in floral stem cell termination. Genetic evidence suggests that *AGO10* acts to terminate floral stem cells in part by facilitating miR172-mediated repression of *AP2*. We demonstrate that the HD-Zip genes *PHABULOSA* (*PHB*) and *PHAVOLUTA* (*PHV*), targets of miR165/166 [29,30], play a previously unknown yet crucial role in the proper termination of floral stem cells. Like AGO1, AGO10 associates with miR172 and miR165/166 *in vivo* and exhibits slicing activity *in vitro*. Intriguingly, AGO1 and AGO10 exert opposite effects on miR165/166 *in vivo*, yet both contribute to the termination of floral stem cells.

Results

AGO10 promotes floral determinacy

To identify genes with functions similar to those of *AG* in promoting stamen/carpel identities and terminating floral stem cells, we performed ethyl methanesulfonate (EMS) mutagenesis to screen for enhancers of the *hua1-1 hua2-1* double mutant, which will be hereafter referred to as *hua1 hua2*. *hua1 hua2* flowers are largely normal except that the gynoecia are shorter and more enlarged at the apical end than wild type (Figure 1A). The floral phenotypes of *hua1 hua2* are sensitive to the dosage of functional *AG*. Combination of *ag-1*/+ or *ag-4* with *hua1 hua2* drastically enhances the homeotic and floral determinacy defects of *hua1 hua2*

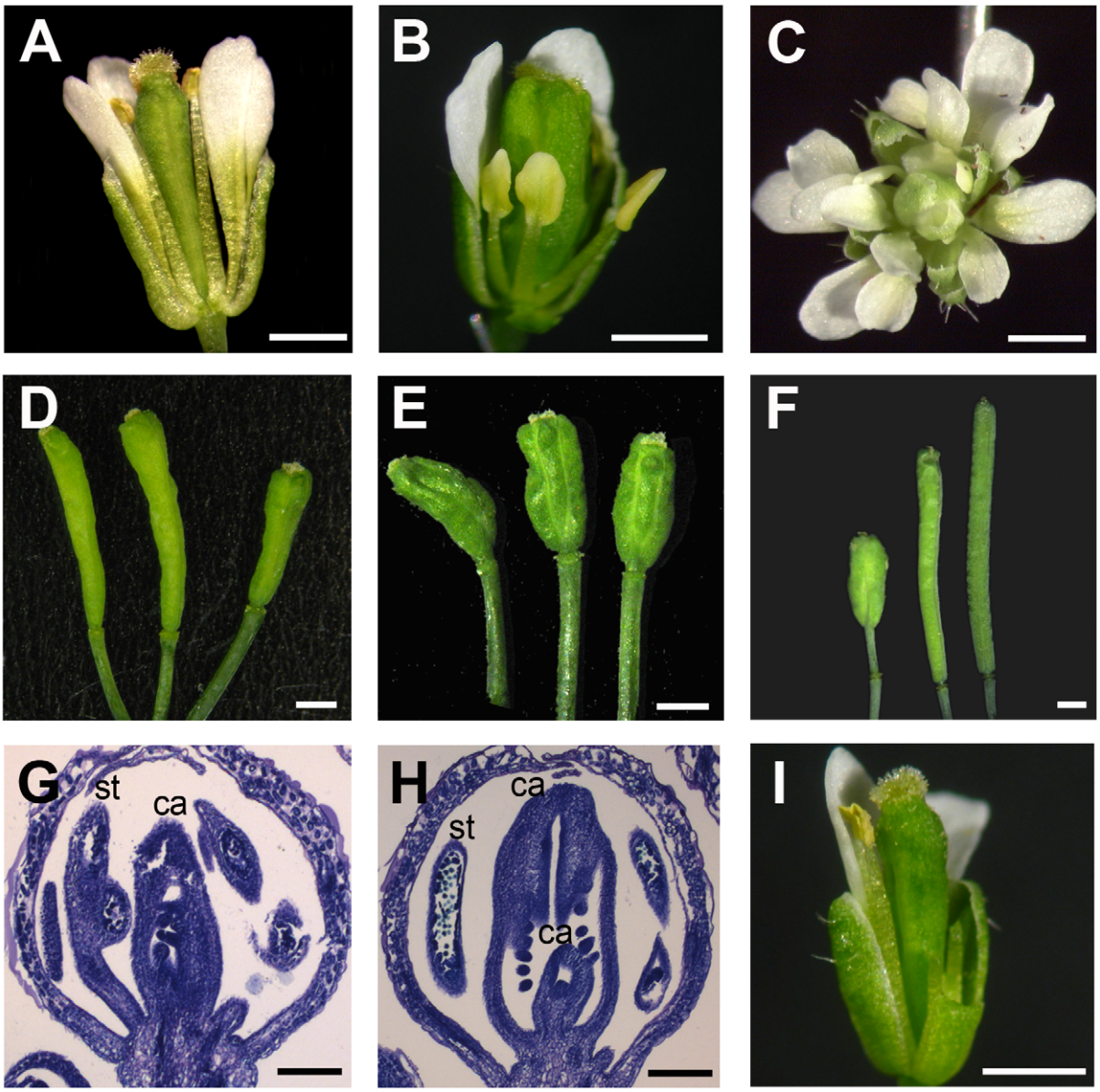

Figure 1. *hen6* (*ago10-12*) and *hen7* (*ag-10*) mutations enhance *hua1 hua2*. (A) A *hua1 hua2* flower with a gynoecium that was slightly enlarged at the top. (B) A *hua1 hua2 hen6* (or *hua1 hua2 ago10-12*) flower with petaloid stamens and a bulged gynoecium containing ectopic floral organs inside. (C) A *hua1 hua2 hen7* (or *hua1 hua2 ag-10*) flower that resembled that of an *ag* null mutant in that the third whorl stamens were transformed into petals and that the sepal-petal-petal pattern was reiterated. (D) Siliques of *hua1 hua2*. (E) Siliques of *hua1 hua2 ago10-12*. (F) A representative silique of *hua1 ag-10* (left), *hua1 ag-10* plants carrying the *pAG::AG-GFP* transgene (middle), and L*er* (right). (G, H) Longitudinal sections of *hua1 hua2* and *hua1 hua2 ago10-12* stages 10-11 flowers. An ectopic floral meristem inside the fourth whorl carpels was present in *hua1 hua2 ago10-12* (H) but not *hua1 hua2* (G). ca, carpel; st, stamen. (I) A *hua1 hua2 ago10-12* flower carrying *AGO10* genomic DNA, which rescued the floral determinacy and homeotic defects of *hua1 hua2 ago10-12*. Some outer whorl organs were removed to expose the gynoecia in (A), (B), and (I). Scale bars, 50 μm in (G), (H) and 1 mm in all other panels.
doi:10.1371/journal.pgen.1001358.g001

[31]. Accordingly, a genetic screen in the *hua1 hua2* background effectively identified genes that promote reproductive organ identity specification or floral determinacy [28,32–35]. Among the new mutations we isolated in this screen were *hua enhancer6* (*hen6*) and *hua enhancer7* (*hen7*), recessive alleles in two genes.

hen6 enhanced the floral phenotypes of *hua1 hua2* in terms of both reproductive organ identities and floral determinacy. While *hua1 hua2* flowers have stamens in the third whorl, petaloid stemens were observed in *hua1 hua2 hen6* flowers (Figure 1A,1B; Figure S3H), indicating a defect in stamen identity specification. In addition, *hua1 hua2 hen6* gynoecia were much shorter than those of *hua1 hua2* and appeared bulged or heart-shaped (Figure 1B,1D,1E). Extra floral organs internal to the fourth whorl carpels were present in *hua1 hua2 hen6* but not in *hua1 hua2* gynoecia; these extra organs were generated from an indeterminate floral meristem as observed in longitudinal sections of flowers (Figure 1G,1H; Table S1). *hen6* was mapped to the BAC MQD19 on chromosome 5, from which *AGO10* was selected as a candidate gene for sequencing. A C-to-T transition leading to the substitution of leucine (L) 674, which is highly conserved among all *Arabidopsis* AGO proteins, by phenylalanine (F) was found in *AGO10* (Figure S1A,S1B). The homeotic and floral determinacy defects of *hua1*

hua2 hen6 were rescued by *AGO10* genomic DNA and the fully rescued plants appeared morphologically identical to *hua1 hua2* (Figure 1I). Therefore, *hen6* was renamed *ago10-12*. While many previously isolated *ago10* alleles show SAM defects with incomplete penetrance, the *ago10-12* single mutant had no obvious SAM defects, suggesting that the L674F mutation does not completely compromise *AGO10* function.

hen7 strongly enhanced *hua1 hua2* such that *hua1 hua2 hen7* flowers resembled those of *ag* null mutants. Stamens were transformed to petals and the floral meristems failed to terminate (Figure 1A,1C). Rough mapping showed that *hen7* was linked to *AG*, and sequencing of *AG* revealed a G-to-A mutation resulting in an glutamate (E)-to-lysine (K) substitution at the 144th amino acid (Figure S1A). To show that *AG* could rescue the *hen7* mutant phenotypes, we utilized the fertile *hua1 hen7* double mutant. *hua1 hen7* flowers had no organ identity defects, but the gynoecia were bulged with secondary floral organs inside the primary carpels (Figure 1F; Table S1). The floral determinacy defects of *hua1 hen7* flowers could be rescued by a *pAG::AG-GFP* construct (Figure 1F). Therefore, *hen7* is an *ag* allele, which we named *ag-10*. The *ag-10* single mutant flowers had a normal complement of floral organs as in wild type (Figure 2A); as such, it is the weakest *ag* allele known to date. Most siliques on an *ag-10* plant, however, can be distinguished from wild type by their curvature (Figure 2D). A small proportion of siliques were slightly bulged with additional organs inside (Figure 2D; Table S1). This contrasted with *hua1 ag-10* plants, in which all siliques were bulged with internal floral organs inside (Table S1). Therefore, *ag-10* was mildly defective in floral determinacy and this defect was drastically enhanced by *hua1*.

We performed another EMS screen in the *hua1 ag-10* background to identify mutants with enhanced floral determinacy defects. One mutant had a flowers-within-flower phenotype reminiscent of *ag* null mutants. After removal of the *hua1* mutation by crossing, the double mutant of *ag-10* and the enhancer mutation still exhibited strong floral determinacy defects; all siliques on the double mutant were severely bulged and ectopic floral organs were present inside the primary carpels (Figure 2B,2E; Table S1). Flowers of the double mutant did not exhibit any homeotic transformation and were fertile. We noticed that seedlings of the double mutant exhibited SAM defects at a low penetrance similar to *ago10* alleles. This, together with the mapping of the mutation to the top of chromosome 5, led us to suspect that the enhancer mutation was in *AGO10*. Sequencing *AGO10* from the double mutant identified a G-to-A mutation that introduced a premature stop codon close to the end of the second exon of *AGO10* (Figure S1A). Introduction of a *pAGO10::AGO10-FLAG* construct into the double mutant fully rescued the floral determinacy defect (Figure 2C). Therefore, we named this mutation *ago10-13*. From longitudinal sections, it was clear that the floral meristems persisted well beyond stage 6 in all *ag-10 ago10-13* flowers but not in most *ag-10* flowers (Figure 2G,2H), suggesting that *AGO10* is required for floral stem cell termination. Like other *ago10* alleles, the gynoecia and siliques of the *ago10-13* single mutant were shorter and wider than wild type (Figure S3A,S3B).

In an EMS screen in the *ag-10* background, we identified yet another *ago10* allele, *ago10-14*, which harbored a G-to-A mutation that changes the 731th amino acid from aspartic acid (D) to asparagines (N) (Figure S1A). Flowers of *ag-10 ago10-14* resembled those of *ag-10 ago10-13* in that the gynoecia were bulged (data not shown). The following genetic and molecular studies were performed mainly with *ago10-12* and *ago10-13* alleles.

Given that *ago10-12* enhanced *hua1 hua2* and both *ago10-13* and *ago10-14* enhanced *ag-10* in terms of floral determinacy, we conclude that *AGO10* promotes floral stem cell termination. Consistent with such a role, the YFP-ZLL fusion protein from the functional *pZLL::YFP-ZLL* transgene [36] was found in the center of stages 5-6 floral meristems by immunolocalization (Figure 3A). By stage 7, YFP-ZLL was found on the adaxial side of carpel primordia (Figure 3B).

AGO10 terminates floral stem cells through repression of *WUS* expression

To investigate how *AGO10* regulates floral stem cells, we examined the genetic interactions between *ago10* alleles and mutations in key stem cell regulators. In *wus-1*, the floral meristems are terminated prematurely, resulting in incomplete flowers with four sepals, four petals, and typically a single stamen [2] (Figure S3E). *hua1 hua2 ago10-12 wus-1* flowers had identical phenotypes to those of *wus-1* in terms of floral determinacy (Figure 4A), indicating that *wus-1* was epistatic to *hua1 hua2 ago10-12*. Unlike *wus-1* (Figure S3E), the single stamen in *hua1 hua2 ago10-12 wus-1* was petaloid as in *hua1 hua2 ago10-12* (Figure 4A), indicating that the homeotic transformation of stamens into petaloid stamens in *hua1 hua2 ago10-12* was independent of *WUS*. Similarly, *wus-1* was epistatic to *ag-10 ago10-13* in terms of floral determinacy (data not shown). Therefore, *AGO10* acts through *WUS* to regulate floral meristem activity. This conclusion was also supported by the prolonged expression of *WUS* in floral meristems caused by *ago10* mutations. Using *in situ* hybridization, we found that *WUS* expression in *hua1 hua2 ago10-12* flowers persisted well beyond floral stage 6, when *WUS* expression was terminated in *hua1 hua2* flowers (Figure 3E,3F). Similarly, *WUS* expression was detected in very old *ag-10 ago10-13* but not *ag-10* flowers (Figure 3G,3H).

CLV3 controls the spatial domain of *WUS* expression and the size of the stem cell domain [37]. *clv3-1* flowers contain extra floral organs of all types, particularly stamens and carpels, due to enlarged floral meristems [38]. The combination of *hua1 hua2 ago10-12* and *clv3-1* had a synergistic effect on floral determinacy. The gynoecia of the quadruple mutant generated a massive amount of stigmatic tissue bursting out of the primary carpels (Figure S3F,S3G). Similar phenotypes were observed for *ag-10 ago10-13 clv3-1* flowers (data not shown), implying that *AGO10* and *CLV3* act largely independently.

Since *AG* is crucial in the termination of floral stem cells, we evaluated the relationship between *AG* and *AGO10* through extensive genetic interaction studies. We first introduced the null *ag-1* allele into *hua1 hua2 ago10-12*. The quadruple mutant flowers were initially similar to *ag-1* flowers, but the meristems continued to develop and appeared fasciated in old flowers (data not shown). Given that *ago10-12* was a weak allele, we next combined the stronger *ago10* alleles *pnh-1* [25] or *ago10-13* with *ag-1*. Most flowers of the *ag-1 pnh-1* and *ag-1 ago1-13* double mutants appeared more fasciated than *ag-1* flowers (Figure 4B,4C; data not shown). The mild enhancement implies that *AGO10* acts through the *AG* pathway to repress *WUS* expression but that *AGO10* also has an *AG*-independent function in floral stem cell regulation. We conducted *in situ* hybridization to examine the patterns of *AG* expression in *ag-10* and *ag-10 ago10-13* flowers. *AG* transcripts were detected in the inner two whorls of *ag-10* and *ag-10 ago10-13* floral meristems (Figure 3C,3D). Therefore, *ago10-13* did not affect the spatial domain of *AG* expression or lead to obvious changes in *AG* mRNA levels in floral meristems.

AGO1 is also required for floral stem cell termination

Since *AGO1* is the most closely related to *AGO10* among the ten *Arabidopsis AGO* genes, we sought to determine whether *AGO1* is also required for floral stem cell termination. We introduced the

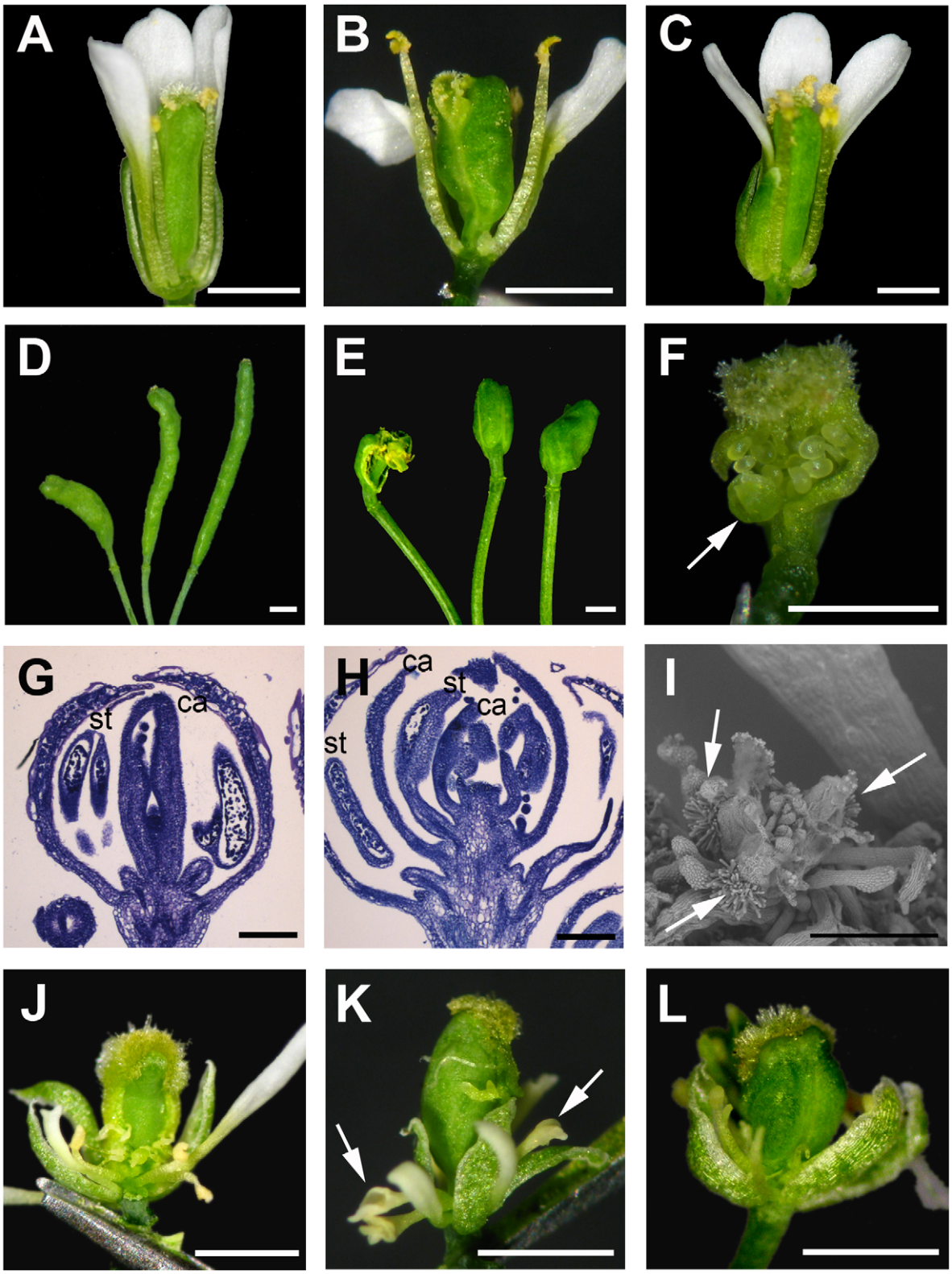

Figure 2. *AGO10* and *AGO1* promote floral determinacy. (A) An *ag-10* flower; most *ag-10* flowers were similar to wild-type ones. (B) An *ag-10 ago10-13* flower; the gynoecia of *ag-10 ago10-13* flowers were bulged and contained ectopic floral organs internally. (C) A flower of *ag-10 ago10-13 pAGO10::AGO10-FLAG* showing that *AGO10* rescued the floral determinacy defects of *ag-10 ago10-13*. (D) Representative siliques from *ag-10* plants. Most were similar to wild-type siliques, while some were constricted on one side but still long and thin. Bulged siliques with internal floral organs (represented by the one on the left) were observed at a low frequency (usually 1-2 per plant). (E) Siliques from *ag-10 ago10-13* plants. 100% of the siliques on an *ag-10 ago10-13* plant were bulged. Occasionally, the primary carpels that make up a silique were not properly fused, revealing the internal organs. (F) An *ago10-13 ago1-11/+* gynoecium with internal floral organs (arrow) bursting out of the gynoecium. (G, H) Longitudinal sections

of stage 12 *ag-10* and *ag-10 ago10-13* flowers. The floral meristem was not visible in most *ag-10* flowers (G), whereas it was still active in *ag-10 ago10-13* flowers to result in extra whorls of organs inside the fourth whorl carpels (H). ca, carpel; st, stamen. (I) A scanning electron micrograph of an *ago1-11 ago10-13*/+ flower. The severe floral determinacy defects were reflected by the presence of numerous floral organs inside unfused primary carpels (indicated by arrows). (J–L) *ago1-11* enhanced the floral determinacy defects of *hua1 hua2* and *ag-10*. (J) An *ago1-11* flower. (K) A *hua1 hua2 ago1-11* flower with bulged gynoecia and petaloid stamens (arrows). (L) A representative *ag-10 ago1-11* flower with a severely bulged gynoecium. In (A), (B), (C), and (J), some outer whorl floral organs were removed to expose the gynoecia. Scale bars, 50 μm in (G) and (H), 500 μm in (I), and 1 mm in all other panels.
doi:10.1371/journal.pgen.1001358.g002

partial loss-of-function *ago1-11* mutation [39] into *hua1 hua2* and *ag-10*. The infertile *ago1-11* flowers develop all four types of floral organs, although the organs are abnormal in morphology (Figure 2J; Figure S3C). In *hua1 hua2 ago1-11* flowers, either the gynoecia were severely bulged or the carpels were completely unfused with ectopic flowers developing internal to the primary carpels (Figure 2K). Similarly, indeterminate phenotypes were observed in the *ag-10 ago1-11* double mutant (Figure 2L). Therefore, *AGO1*, like *AGO10*, is required for floral stem cell termination.

Genetic studies conducted by others as well as by ourselves show that *AGO1* and *AGO10* have overlapping functions in terminating floral meristems. First, it was previously shown that combining the strong *ago1-7* and *pnh-2* (an *ago10* allele) alleles resulted in embryo lethality [23]. But *ago1-7*/+ *pnh-2*/*pnh-2* and *ago1-7*/*ago1-7 pnh-2*/+ flowers showed an increase in the number of floral organs as well as ectopic growth of tissues inside the primary carpels (i.e., loss of floral determinacy). Second, we crossed the weak *ago1-11* allele with the strong *ago10-13* allele but also failed to obtain viable double mutants. The *ago1-11 ago10-13*/+ plants were smaller than *ago1-11* in stature. Some inflorescences harbored flowers with filamentous floral organs and obviously enlarged floral meristems (Figure S3D). When carpels were formed, they were unfused and additional floral organs were observed inside the primary carpels (Figure 2I). In *ago10-13 ago1-11*/+ plants, the gynoecia were bulged and additional floral organs were found in some of the gynoecia upon dissection (Figure 2F). In summary, both *ago1 ago10*/+ or *ago1*/+ *ago10* plants were more severe in floral determinacy defects than the corresponding single mutants. The dosage effects of *ago1* and *ago10* alleles indicate that the two genes have overlapping functions in floral stem cell termination.

AGO10 acts partly through miR172 to promote floral determinacy

miR172 negatively regulates *AP2* mainly through translational repression [10,11] to result in proper floral patterning including the termination of floral stem cells [12] and stamen identity specification [32]. In the *hua1 hua2* background in which *AG* expression is reduced, loss of function in *HEN1*, a player in miRNA biogenesis [40], results in stamen-to-petal transformation. The homeotic transformation is mainly due to de-repressed *AP2* expression since the *ap2-2* mutation restores stamen identity to *hua1 hua2 hen1-1* flowers [32].

To determine whether *AGO10* acts through miR172 in floral patterning, we examined the genetic interactions between *ago10* and *ap2* mutations by generating *hua1 hua2 ago10-12 ap2-2* and *ag-10 ago10-13 ap2-2*. First, *ap2-2* suppressed the homeotic defects of *hua1 hua2 ago10-12* in that the third whorl petaloid stamens in the

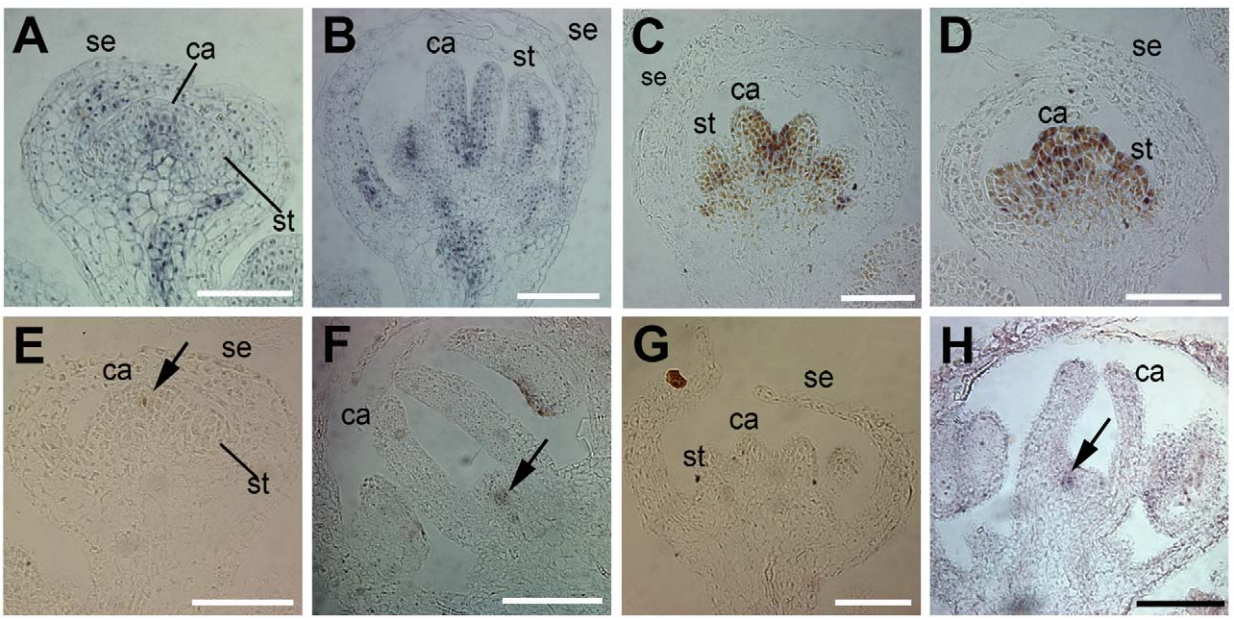

Figure 3. Expression patterns of *AGO10*, *AG*, and *WUS* in floral meristems. (A, B) Immunolocalization of AGO10 protein using anti-GFP antibodies in *zll-1 pZLL::YFP-ZLL* flowers. The grey signals represent AGO10. Before floral stage 6, AGO10 was predominantly localized at the floral meristem and in provascular tissue (A); AGO10 was adaxialized in carpels beyond stage 6 (B). (C, D) The *ago10-13* mutation did not alter the spatial patterns of *AG* expression in developing flowers. *AG* mRNA was similarly present in the inner two whorls of an *ag-10* (C) and an *ag-10 ago10-13* (D) flower at stages 6–7. (E–H) *ago10* mutations led to prolonged *WUS* expression. In *hua1 hua2*, the latest stage when *WUS* mRNA could be detected was stage 6 (E). *WUS* expression persisted to stages 8-9 in *hua1 hua2 ago10-12* flowers (arrow in F). *WUS* expression was diminished by stage 7 in *ag-10* (G). In *ag-10 ago10-13*, *WUS* expression could be observed in stages 8–9 flowers (arrow in H). Scale bars, 50 μm. ca, carpel; se, sepal; st, stamen.
doi:10.1371/journal.pgen.1001358.g003

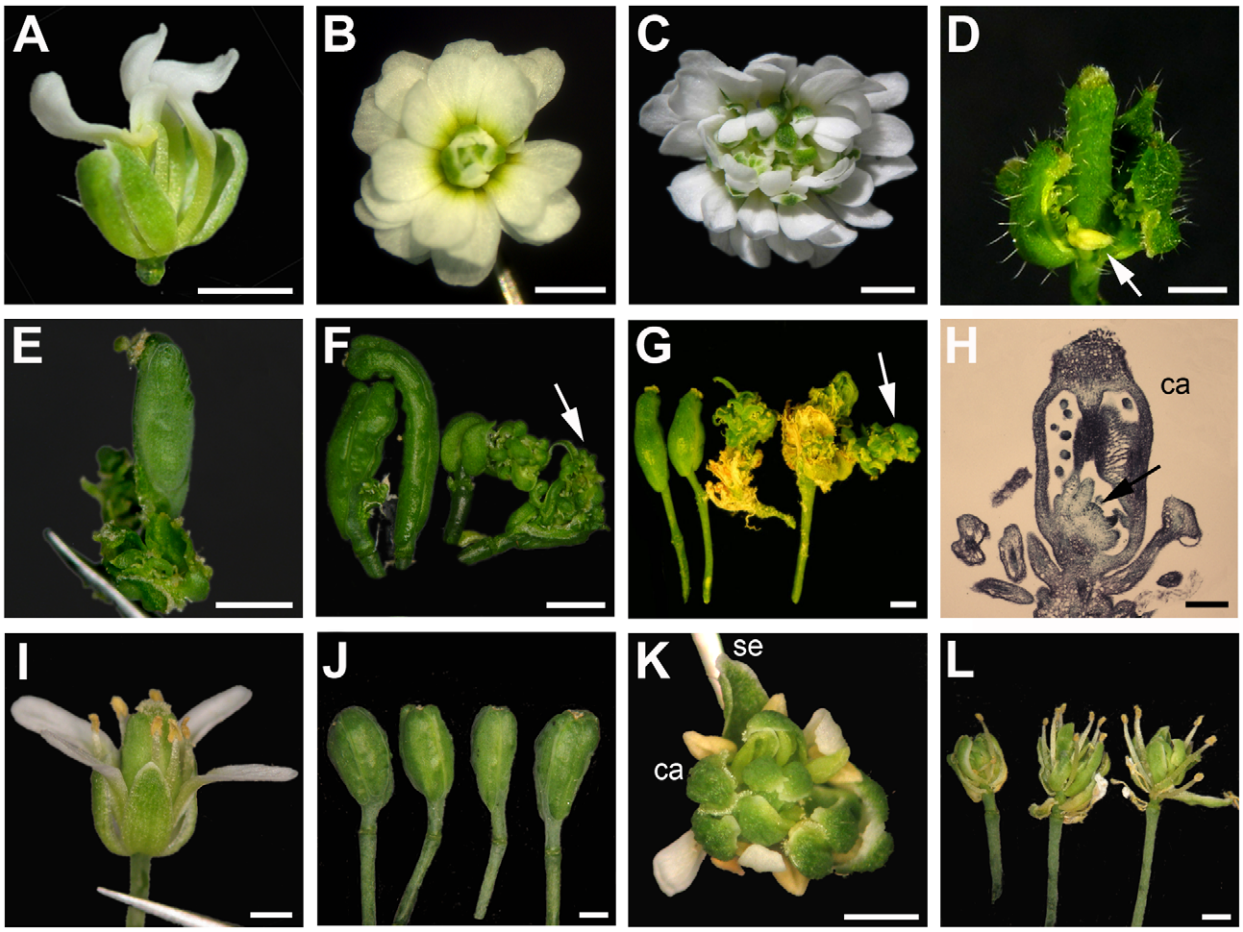

Figure 4. Genetic interactions between *AGO10* and meristem regulators. (A) A *hua1 hua2 ago10-12 wus-1* flower. *wus-1* was completely epistatic to *hua1 hua2 ago10-12* in floral determinacy such that the quadruple mutant flower had an incomplete set of floral organs as in a *wus-1* flower. (B) An *ag-1* flower. (C) An *ag-1 pnh-1* flower that had apparently more floral organs than an *ag-1* flower and showed signs of fasciation. (D,E) *ap2-2* partially suppressed the floral determinacy defects of *hua1 hua2 ago10-12* and *ag-10 ago10-13*. (D) A representative of the non-bulged gynoecia of some *hua1 hua2 ago10-12 ap2-2* flowers. The petaloid stamens in *hua1 hua2 ago10-12* were rescued back to stamens (arrow) by the *ap2-2* mutation. (E) A representative of *ag-10 ago10-13 ap2-2* gynoecia, which are longer than *ag-10 ago10-13* gynoecia (Figure 2E). (F–H) *phb-1d* and *phv-5d* each enhanced the determinacy defects of *ag-10*. (F) *ag-10 phb-1d/+* siliques. Ectopic floral organs, indicated by the arrow, were found in the siliques of most *ag-10 phb-1d/+* flowers. (G) *ag-10 phv-5d* siliques were bulged or contained ectopic floral organs, as indicated by the arrow. (H) A longitudinal section of an *ag-10 phb-1d/+* gynoecium. An ectopic floral meristem (indicated by the arrow) could be observed inside the carpels. (I–L) *ag-10* plants harboring transgenic amiR165/166 exhibited loss of floral determinacy. (I–J) Weaker determinacy defects of some *ag-10* amiR165/166 plants. The gynoecia were bulged as in *ag-10 ago10-13*. (K–L) Stronger determinacy defects of some *ag-10* amiR165/166 plants. The gynoecia were replaced by an internal flower. Scale bars, 50 μm in (H), and 1 mm in all other panels. ca, capel; se, sepal.
doi:10.1371/journal.pgen.1001358.g004

triple mutant were restored to stamens in the quadruple mutant (Figure 4D). While the third whorl organs in *hua1 hua2 ago10-12* had patches of cone-shaped cells reminiscent of petal epidermal cells (Figure S3I, S3J), the third whorl organs in *hua1 hua2 ago10-12 ap2-2* had epidermal cells with the shapes of interlocking puzzle pieces resembling anther epidermal cells (Figure S3K,S3L). This indicates that the homeotic transformation in *hua1 hua2 ago10-12* flowers is due to de-repressed *AP2* and that *AGO10* mediates the function of miR172 in repressing *AP2*. Second, *ap2-2* partially suppressed the floral determinacy defects of *hua1 hua2 ago10-12* and *ag-10 ago10-13* flowers. *ap2-2* did not affect the shapes of *hua1 hua2* or *ag-10* gynoecia ([31]; Figure S3M), but caused *hua1 hua2 ago10-12* and *ag-10 ago10-13* gynoecia to be less bulged (compare Figure 4D to Figure 1B and Figure 4E to Figure 2E), suggesting that the determinacy defects were not as severe as in *hua1 hua2 ago10-12* or *ag-10 ago10-13*. To quantify this effect, we dissected gynoecia to observe the presence/absence of ectopic organs inside. Compared with *hua1 hua2 ago10-12* and *ag-10 ago10-13* plants that had ectopic floral organs in 91% and 100% of the siliques, respectively, *ap2-2* reduced the percentage of siliques with internal organs to 41% and 86% in *hua1 hua2 ago10-12* and *ag-10 ago10-13*, respectively (Table S1). Although the suppression effect for the latter genotype was not large, we found that *ap2-2* completely suppressed the presence of an elongated gynophore in *ag-10 ago10-13* (Figure S3N-S3P). An elongated gynophore probably reflects a partial conversion of the floral meristem to an inflorescence meristem, hence, prolonged stem cell activity. Therefore, the floral stem cell defects of *ago10* mutants were partially rescued by *ap2-2*, indicating that *AP2* is likely de-repressed in *ago10* mutants and that the de-repression is partially responsible for the floral stem cell defects. This conclusion is consistent with the similar genetic behavior of *AP2m3* and *ago10* in that both enhanced *ag-1* ([12]; Figure 4B,4C).

Despite the genetic evidence supporting de-repressed *AP2* expression in *ago10* mutants, we were unable to consistently detect an increase in AP2 protein levels in *ag-10 ago10-13* vs. *ag-10* or

ago10-13 vs. wild type by western blotting (data not shown). This is likely attributable to insufficient sensitivity of the assay in the detection of small differences. Since the levels of miR172 were not affected by *ago10-13* (Figure S2A), it is likely that miR172-mediated repression of *AP2* requires *AGO10*.

AGO10 is associated with miRNAs *in vivo*

Although our genetic evidence indicates that *AGO10* mediates the activities of miR172 and previous genetic studies implicate *AGO10* in mediating the translational repression of target mRNAs by multiple miRNAs [26], molecular evidence of AGO10 acting directly with miRNAs has been lacking. We sought to determine whether AGO10 was associated with miRNAs *in vivo*. We immunoprecipitated (IP) YFP-ZLL from inflorescences of *zll-1 pZLL::YFP-ZLL* plants [36] with anti-GFP antibodies. *pAG::AG-GFP* and L*er* (wild type) were used as a positive and a negative control, respectively, for the IP. Proteins of the expected sizes from the *pZLL::YFP-ZLL* and *pAG::AG-GFP* IP samples were detected by western blotting (Figure 5A). We also included *pAGO1::FLAG-AGO1* [20] and Col (a control for *pAGO1::FLAG-AGO1*) for comparison. We extracted RNAs from the IP samples and performed small RNA northern blotting to detect selected miRNAs and siRNAs. AGO10 bound miRNAs such as miR165/166, miR172, miR173, miR319 and miR168 (Figure 5B), but not miR390 (Figure S4), which specifically associates with AGO7 [18]. Northern blotting failed to detect signals for 24 nt endogenous siRNAs from several loci from the IP samples (data not shown). The AGO10-associated miRNAs are also associated with AGO1 *in vivo* (Figure 5B; [17,20]).

AGO10 has "slicer" activity

Because AGO10 contains the DDH catalytic residues that are critical for the "slicer" activity of AGO proteins, we decided to determine whether AGO10 is catalytically active *in vitro*. We performed a "slicer" activity assay on the miR165/166 target *PHABULOSA* (*PHB*). A portion of the *PHB* transcript containing the miR165/166 binding site was generated through *in vitro* transcription and incubated with IP samples from *pAGO1::FLAG-AGO1* and *pZLL::YFP-ZLL* plants as well as the corresponding negative controls Col and *pAG::AG-GFP*, respectively. A miR165/166-resistant *PHB* transcript, *PHBm*, was also included as a negative control. The *PHB* transcript was cleaved into two fragments of expected sizes by both FLAG-AGO1 and YFP-ZLL but not by the corresponding control IPs (Figure 5C). As expected, the *PHBm* transcript failed to be cleaved by either FLAG-AGO1 or YFP-ZLL (Figure 5C). This shows that AGO10, like AGO1, can cause the cleavage of miRNA-targeted mRNAs.

Given that AGO10 has "slicer" activity, we next examined the levels of small RNA-targeted mRNAs in *ago10* mutants. The levels of most examined mRNAs were not obviously different between *ago10-13* and wild type (Figure S2B), consistent with findings from a previous study [26]. A small elevation in the levels of *CUC1* mRNA, which is targeted by miR164, was consistently detected in *ago10-13* (Figure S2B). Interestingly, a small reduction in the levels of miR164 in *ago10* mutants was consistently observed (Figure S2A). The miR164-resistant *CUC1* transgene (*pCUC1::CUC1m-GFP*; [41]) did not enhance the determinacy defects of *ag-10* (data not shown), suggesting the *ag-10 ago10-13* floral determinacy defects were unlikely attributable to de-repressed *CUC1* expression. There are several explanations for the lack of differences in miRNA target mRNA levels between *ago10* and wild type. First, changes are masked by the target mRNAs outside of the highly restricted expression domains of *AGO10*. Second, *AGO1* is sufficient to regulate most miRNA-targeted mRNAs at the transcript level, and AGO10 acts primarily through translational inhibition *in vivo*.

miR165/166 and its targets, the HD-Zip genes, are crucial players in floral determinacy

The fact that the *ap2-2* mutation failed to completely suppress *hua1 hua2 ago10-12* or *ag-10 ago10-13* suggests that *AGO10* regulates floral stem cell termination also through other miRNAs. Because AGO10 associates with miR165/166 and the HD-Zip genes *PHB*, *PHAVOLUTA* (*PHV*), and *REVOLUTA* (*REV*) targeted by this miRNA strongly influence the formation of the SAM [29], we tested whether proper regulation of *PHB* by miR165/166 was crucial for floral stem cell termination. We crossed the miR165/166-resistant form of *PHB*, *phb-1d* [42], with *ag-10 ago10-13*. Both *ag-10 phb-1d*/+ and *ag-10 ago10-13*/+ *phb-1d*/+, but not *phb-1d*/+ flowers had bulged gynoecia with ectopic floral organs inside (Figure 4F; Figure S3Q,S3R). Sections of *ag-10 phb-1d*/+ flowers revealed indeterminate floral meristems inside the primary carpels (Figure 4H). In addition, in the genetic screen in the *ag-10* background, we isolated a semi-dominant *phv* allele, *phv-5d*, as an *ag-10* enhancer. The *ag-10 phv-5d* double mutant exhibited bulged siliques throughout the plant (Figure 4G) whereas most but not all siliques in *ag-10 phv-5d*/+ plants were bulged (Figure S3S). *phv-5d* contained a G-to-A mutation in the miR165/166 binding site (Figure S1A,S1C) and this lesion was identical to those of the previously characterized *phv-1d*, *-2d*, *-3d*, and *-4d* alleles [29]. Although the mutation resulted in a glycine-to-aspartic acid substitution, extensive studies of an identical mutation in *PHB* (*phb-3d*) showed that it was the disruption of miR165/166 targeting rather than the amino acid change that caused the developmental defects in *phb-3d* [30]. Collectively, these results demonstrate that miR165/166-mediated regulation of HD-Zip genes is necessary for floral stem cell termination.

Having shown that the repression of *PHB* and *PHV* by miR165/166 is important for floral stem cell termination, we sought to determine whether *ago1* or *ago10* mutations resulted in defects in miR165/166-mediated repression of HD-Zip genes. We first examined the accumulation of miR165/166 in *ago1-11*, *ago1-11 ago10-13*/+, *ago10-13*, and *ago1-11*/+ *ago10-13* inflorescences. Intriguingly, miR165/166 levels were reduced in *ago1-11* but increased in *ago10-13* (Figure 5D). The increase in miR165/166 levels was consistently observed in all *ago10* alleles tested (*ago10-12*, *ago10-13*, and *pnh-1*; Figure S2A and data not shown), and was also previously observed in *ago10* seedlings [43].

Next, we examined the levels of HD-Zip mRNAs in L*er*, *ago10-13*, *ago1-11*, *ag-10*, and *ag-10 ago10-13* flowers by realtime RT-PCR. The levels of *PHB*, *PHV* and *CORONA* (*CNA*) mRNAs were reduced in *ago10* genotypes as compared to controls (Figure 5E,5F), which correlated with the increased abundance of miR165/166. This indicated that *AGO1* was sufficient to control the mRNA levels of the HD-Zip genes in the absence of *AGO10*. In *ago1-11*, in which miR165/166 levels were low, *PHB* and *PHV* mRNA levels were slightly higher than wild type (Figure 5E), consistent with AGO1 being the major slicer of *PHB* and *PHV in vivo*. Therefore, *ago1* and *ago10* mutations have opposite effects on miR165/166 accumulation and expression of the HD-Zip genes.

ago10 mutants were previously found to have increased levels of miR165/166 in seedlings and the increase in miR165/166 and the resulting decrease in HD-Zip expression were responsible for the SAM and leaf polarity defects of *ago10* mutants [43]. Therefore, it is possible that reduced HD-Zip expression caused by elevated levels of miR165/166 also underlies the floral determinacy defects of *ago10* mutants. However, it is also possible that *AGO10* regulates the HD-Zip genes through translational repression since it is

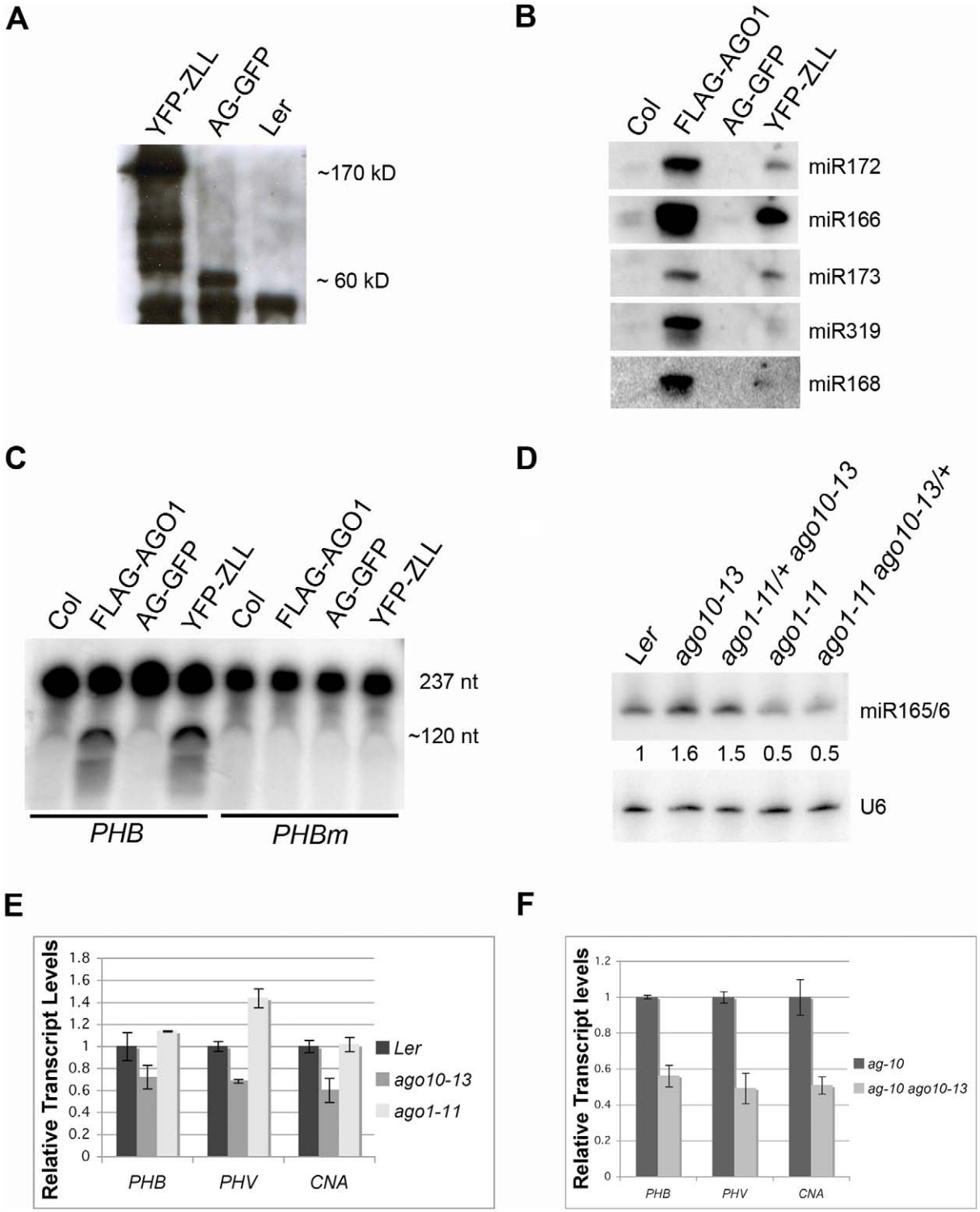

Figure 5. AGO10 is associated with miRNAs *in vivo* and is catalytically active as a ''slicer'' *in vitro*. (A) Immunoprecipitation (IP) followed by western blotting using anti-GFP antibodies from three genotypes as indicated. The immunoprecipitated YFP-ZLL fusion protein could be detected as a band of the expected size (~170 kD). AG-GFP (~60 kD) and L*er* served as a positive and a negative control for the IP, respectively. (B) Detection of miRNAs by northern blotting from FLAG-AGO1 and YFP-ZLL IP. Col and AG-GFP served as negative controls for FLAG-AGO1 and YFP-ZLL, respectively. (C) An *in vitro* ''slicer'' assay. Both FLAG-AGO1 and YFP-ZLL immune complexes cleaved the *PHB* wild-type probe, but not the miR165/166-resistant probe. The full-length *PHB* and *PHBm* probes were 237 nt. The 5′ and 3′ cleavage fragments were 112 nt and 125 nt, respectively, and were not separated in the gel (represented by the band of approximately 120 nt). (D) Northern blot for miR165/166 in the genotypes as indicated. U6 served as a loading control. The numbers below the gel image indicate the relative abundance of miR165/166. (E) Expression of the HD-Zip genes *PHB*, *PHV* and *CNA* in wild type (L*er*), *ago10-13*, and *ago1-11* inflorescences as examined by realtime RT-PCR. (F) Realtime RT-PCR to determine the levels of *PHB*, *PHV*, and *CNA* mRNAs in *ag-10* and *ag-10 ago10-13* inflorescences.
doi:10.1371/journal.pgen.1001358.g005

known to do so on other miRNA target genes [26]. If this were the case, the levels of HD-Zip proteins would be increased in *ago10-13* despite the reduction in the mRNA levels. The lack of antibodies against the HD-Zip proteins prevented us from directly determining the levels of HD-Zip proteins in *ago10* mutants. We used the mRNA levels of *LITTLE ZIPPER3* (*ZPR3*), which is a direct target of *PHB* [44], as a proxy for PHB protein levels. It was shown that *ZPR3* mRNA levels are reduced in HD-Zip loss-of-function mutants and increased in miRNA165/166-resistant HD-Zip mutants [44]. Realtime RT-PCR showed that *ZPR3* levels were severely reduced in *ago10-13* (Figure S5), suggesting that HD-Zip protein levels were low in *ago10-13*. Next, we investigated whether reduced HD-Zip gene expression could result in loss of floral determinacy. *ag-10* plants were transformed with an artificial miR165/166 construct in which pre-miR165 and pre-miR166 were placed in tandem and driven by the 35S promoter (Figure S6). Among 64 primary transformants, 16 exhibited premature termination of the SAM, a phenotype reminiscent of *ago10* mutants (Figure S3T). A few of them couldn't survive to generate true leaves. 12 plants exhibited bulged gynoecia similar to *ag-10 ago10* and 4 plants had more severe floral determinacy defects in that the gynoecia were replaced by an internal flower (Figure 4I–4L). This demonstrated that down-regulation of HD-Zip gene expression by over-expression of miR165/166 compromises floral determinacy.

Discussion

AGO10 and AGO1 have similar small RNA–binding specificities but can act differently on miRNAs *in vivo*

Among the ten argonaute proteins in *Arabidopsis*, AGO10 is the most similar in sequence to AGO1, the major miRNA effector. Genetic evidence indicates that *AGO10* and *AGO1* have redundant, overlapping, or even antagonistic functions in development and in RNA silencing [23,27]. For several tested miRNA target genes, protein but not mRNA levels are elevated in *ago10* mutants, suggesting that AGO10 is necessary for miRNA-mediated translational repression of targets [26]. However, direct molecular evidence supporting AGO10 as a miRNA effector has been lacking, perhaps owing to the spatially highly restricted expression of *AGO10*, which makes it challenging to assay small RNA binding and cleavage activities of AGO10. In this study, we provide direct evidence that AGO10 associates with miRNAs *in vivo* and possesses miRNA-directed cleavage activity *in vitro*. So far, three other *Arabidopsis* AGO proteins, AGO1, AGO4 and AGO7, have been shown to possess "slicer" activity [18,20,45]. AGO1 preferentially associates with most miRNAs, ta-siRNAs and transgene siRNAs and mediates target mRNA cleavage and translational inhibition [17,20,26]. AGO7 specifically binds and mediates the function of miR390 in ta-siRNA production through both cleavage and non-cleavage functions [18]. AGO4 binds 24 nt endogenous siRNAs and causes transcriptional silencing of target loci in either a slicer-dependent or slicer-independent manner [45]. From our limited examination of small RNAs bound by AGO10, it appears that AGO10 has similar small RNA binding specificities as AGO1 in that it binds all examined miRNAs except for miR390 and it does not bind 24 nt endogenous siRNAs.

Despite the similar small RNA binding specificities of the two proteins, mutations in the two genes can have different effects on miRNA accumulation and the expression of miRNA target genes. The abundance of many miRNAs is reduced in severe *ago1* mutants [46] but not affected in *ago10* null alleles ([26] and this study). While many miRNA target mRNAs are increased in abundance in *ago1* mutants [21], most assayed miRNA targets are not significantly affected in *ago10* mutants ([26] and this study). miR165/166 is an extreme example of the different effects of *ago1* and *ago10* mutations. While miR165/166 levels are reduced in *ago1-11*, they are increased in *ago10* mutants. The targets of miR165/166 are also affected in opposite directions in the two mutants – they are de-repressed in *ago1-11* and further repressed in *ago10*. This shows that AGO1 is the major slicer acting upon the HD-Zip mRNAs *in vivo*, although AGO10 has slicer activity *in vitro*. While the two argonaute proteins act differently on miR165/166, they both mediate the activities of miR172. Both *ago1-11* and *ago10-12* result in petaloid stamens in the *hua1 hua2* background, suggesting that both *ago1* and *ago10* mutations lead to de-repression of *AP2*. Therefore, AGO1 and AGO10 mediate the activities of some miRNAs but also have different effects on others.

Floral stem cell termination versus differentiation

Floral stem cell termination is tightly coupled to the formation of carpel primordia in flower development. *AG*, which specifies carpel identities, acts to terminate the floral stem cells. It may thus be presumed that the termination of floral stem cells is simply via differentiation of these cells into carpel cells. However, the fact that *ag-10 ago10-13* and *hua1 hua2 ago10-12* flowers have 4th whorl carpels but are indeterminate indicates that carpel identity specification and floral stem cell termination, although both directed by *AG*, are two separable processes. It is expected that factors acting downstream of *AG* in the two processes must be distinct. *KNUCKLES*, for example, is a target of *AG* that is only required for floral determinacy specification [47].

HD-Zip genes, targets of miR165/166, are crucial for the temporal program of floral stem cells

Our previous studies show that both miR172 and its target *AP2* regulate the temporal program of floral stem cells. Plants expressing miR172-resistant *AP2* cDNA have prolonged *WUS* expression and indeterminate floral meristems that produce numerous stamens [12]. In this study, we show that the HD-Zip genes, which are targets of miR165/166 and which are previously known to specify adaxial identity in lateral organs, are also crucial factors in floral stem cell regulation. Over expression of miR165/166 in the *ag-10* background results in indeterminate flowers. Consistent with this, the *phb phv cna* triple mutant was observed to have occasional flowers with enlarged gynoecia containing ectopic carpels inside [48]. On the other hand, *ag-10 phb-1d*/+ and *ag-10 phv-5d* gynoecia are also indeterminate. Given the similar phenotypes of de-repressed *PHB* or *PHV* and loss of function in *PHB*, *PHV* and *CNA* in terms of floral determinacy, it is likely that either too much or too little HD-Zip activity is detrimental to the precise regulation of floral stem cells. Given that the HD-Zip genes promote adaxial identities of lateral organs, our findings raise the intriguing possibility that floral stem cell termination depends on correct polarity specification of the fourth whorl organs. This hypothesis will be tested in the future.

AGO10 and *AGO1* promote floral stem cell termination via similar and different mechanisms

The relationship between *AGO10* and *AGO1* varies depending on the developmental processes. During embryogenesis, *AGO10* and *AGO1* share overlapping functions in maintaining *STM* expression [23]. In the weak *zll-15* mutant background, increasing the dosage of *AGO1* suppressed the defects in embryonic stem cells, while reducing *AGO1* dosage enhanced the defects [27]. Our studies provide the molecular evidence supporting the overlapping biological roles of *AGO1* and *AGO10* by showing that they have

similar small RNA binding specificities and that they both have "slicer" activity. A previous study also documented that *AGO10* antagonizes *AGO1* function. *ago10* mutations partially suppressed the leaf margin serration phenotype of the hypomorphic *ago1-27* allele [27]. Moreover, defects in transgene PTGS and miRNA-mediated gene silencing in the hypomorphic *ago1* mutant were also restored by *ago10* mutations [27]. The elevated AGO1 protein levels in the double mutants reveal that *AGO10* is a negative regulator of *AGO1* at the translational level. By showing that AGO10 binds miR168, which targets *AGO1*, we provide the molecular evidence for the direct regulation of *AGO1* by *AGO10* through miR168.

Our studies support overlapping roles for *AGO10* and *AGO1* in the temporal regulation of floral stem cells but also reveal that the two proteins do so with both similar and different molecular mechanisms (Figure 6). It is well established that *AGO1* mediates the functions of miR172 and miR165/166 in different aspects of plant development. It is likely that *AGO1* promotes floral stem cell termination by repressing *AP2* and HD-Zip expression. Consistent with this, de-repression of *AP2* or HD-Zip genes compromises floral stem cell termination. We show here that AGO10 also associates with these two miRNAs *in vivo*. Genetic evidence suggests that *AGO10* mediates the functions of miR172 in both stamen identity specification and floral determinacy. Therefore, *AGO10* reinforces the functions of *AGO1* in the regulation of *AP2*. Perhaps *AGO1* alone is not sufficient to mediate the functions of miR172 in floral meristems such that *AGO10*, which is specifically expressed in certain cells in the floral meristem, is necessary to act upon the same miRNA. Intriguingly, *AGO1* and *AGO10* exert opposite effects on miR165/166 accumulation and the expression of the HD-Zip genes. The increased miR165/166 levels and reduced expression of HD-Zip genes in *ago10* mutants suggest that *AGO10* promotes HD-Zip gene expression by reducing miR165/166 levels. How *AGO10* does so is currently unknown. Despite the opposite effects on HD-Zip expression, *AGO1* and *AGO10* both promote floral determinacy. This can be reconciled by the fact that both reduced expression and de-repression of HD-Zip genes compromise floral determinacy.

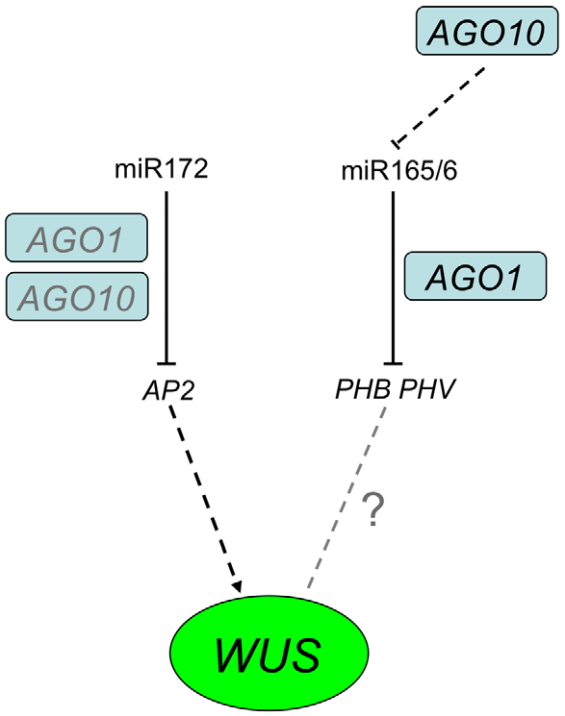

Figure 6. A model of *AGO1* and *AGO10* in floral stem cell regulation. miR172 promotes floral stem cell termination by repressing the expression of *AP2*, which promotes *WUS* expression. Both AGO1 and AGO10 are associated with miR172 *in vivo* and genetic evidence supports a role of AGO10 in mediating the activities of miR172. miR165/166-mediated repression of *PHB* and *PHV* is also necessary for floral stem cell termination. *AGO1* and *AGO10* exert opposite effects on miR165/166. While *AGO1* mediates the activities of miR165/166, *AGO10* represses the expression of miR165/166. The relationship between *PHB*/*PHV* and *WUS* is unknown. Interactions that are potentially indirect are represented by dotted lines.
doi:10.1371/journal.pgen.1001358.g006

SAM and floral meristems—differences in stem cell maintenance

It has not escaped our attention that loss of function of *AGO10* results in opposite effects in stem cell regulation between the SAM and the floral meristems. While *ago10* mutations lead to premature termination of stem cells in the SAM, they result in prolonged floral stem cell maintenance. A previous study found that over expression of miR165/166 recapitulates the SAM defects of *ago10* mutants [49]. In this study, we show that over expression of miR165/166 recapitulates not only the SAM defects but also the floral stem cell defects of *ago10* mutants. Therefore, over accumulation of miR165/166 and reduced expression of the HD-Zip genes probably underlie the failure to maintain the SAM and to terminate the floral stem cells. How reduced expression of the HD-Zip genes leads to opposite effects in the two types of meristems is currently unknown.

Materials and Methods

Plant strains and EMS mutagenesis

The plant strains used in this study are all in the Landsberg *erecta* (L*er*) ecotype except for *ago1-36 pAGO1::FLAG-AGO1* [20], which is in the Columbia (Col) background. All plants were grown at 23°C under continuous light except for those containing the *phb-1d* mutation, which were grown at 17°C. z*ll-1 pZLL::YFP-ZLL* [36], *clv3-1* [38], *wus-1* [2], *ap2-2* [50], *phb-1d* [42], *hua1-1* [31], *hua2-1* [31], and *pnh-1* [25] were all previously characterized.

ag-10, *ago10-12*, *ago10-13*, *ago10-14* and *phv-5d* were isolated in this study. An EMS mutagenesis screen was carried out in the *hua1 hua2* background as described [32]. Single M2 families were screened and two independent mutants, *hua1 hua2 ago10-12* and *hua1 hua2 ag-10*, with bulged gynoecia and *ag* null mutant-like phenotypes, respectively, were identified. The *ag-10* mutation was recovered from fertile siblings. The two lines were backcrossed to *hua1 hua2* three times to clean up the genetic backgrounds. They were also crossed to either *hua1* or *hua2* to generate *hua1 ago10-12*, *hua2 ago10-12*, *hua1 ag-10* and *hua2 ag-10* double mutants. The *ago10-12* or *ag-10* single mutant was obtained by crossing *hua1 ago10-12* or *hua1 ag-10* to wild type. The *ago10-13* allele was isolated in a separate EMS mutagenesis screen in the *hua1 ag-10* background as a mutation that enhanced the floral determinacy phenotypes of *hua1 ago-10*. The mutant was backcrossed to *ag-10* three times to obtain the *ag-10 ago10-13* double mutant, with which most subsequent analyses were conducted. The *ago10-13* single mutant was obtained by crossing *ag-10 ago10-13* to L*er*. The *ago10-14* and *phv-5d* alleles were isolated in an EMS screen in the *ag-10* background as enhancers of its weak determinacy defects.

Construction of amiR165/166

The amiR165/166 plasmid contains modified pre-miR165 and pre-miR166, two stem-loop structures placed in tandem and

inserted between the 2X 35S promoter and the 35S terminator in a small-sized pOT2 vector (Figure S6). The amiR165 and amiR166 construction was done by two rounds of PCR cloning using a proofreading Taq polymerase and two pairs of long primers (~60–100 nt) engineered to contain a SwaI and a PmeI site, respectively. The two pairs of primers (M0SL-at-miR165-SwaI-PR and M0SL-at-miR165-SwaI-PF or M4SL-at-miR166-PmeI-PR and M4SL-at-miR166-PmeI-PF) covered the entire artificial stem-loop sequences of miR165 or miR166 to minimize errors in the miR165 or 166 duplex regions during the PCR reactions. First, the primers M0SL-at-miR165-SwaI-PR and M0SL-at-miR165-SwaI-PF were used to amplify the pOT2 vector that contains the miR168 backbone. The PCR products were cleaved by SwaI and self-ligated to generate a plasmid that contains pre-miR165. Second, PCR was performed using this plasmid as the template with the primers M4SL-at-miR166-PmeI-PR and M4SL-at-miR166-PmeI-PF. The PCR products were cleaved by PmeI and self-ligated to generate a plasmid containing the tandem pre-miR165 and pre-miR166 sequences. Finally, this plasmid in pOT2 was amplified by a pair of primers (Origin-del-PacI-PF and Origin-del-PacI-PR) that contained PacI sites to delete the plasmid replication origin. The PCR products that contained the amiR165/166 and a chloramphenicol selection marker were introduced into a modified pFGC5941 binary vector through the unique PacI site. Recombinant binary plasmids were verified by DNA sequencing before being used for plant transformation.

RNA extraction and realtime RT-PCR

Total RNAs were extracted from inflorescences or seedlings using TRI Reagent (Molecular Research Center, Cat# TR118) as per manufacturer's instructions. Contaminating DNA was removed by DNase I (Promega, Cat# M610A; Roche, Cat# 04716728001) digestion. cDNA was synthesized from 2 µg total RNAs using reverse transcriptase (Fermentas, Cat# EP0441) and an oligo-dT primer. Quantitative PCR was performed in triplicates on a Bio-Rad IQ cycler apparatus with the iQ SYBR green supermix (Bio-Rad, Cat# 170-8882). The primers used are listed in Table S2.

Small RNA northern blotting

Northern blotting to detect small RNAs was performed as described [40,51]. 5′-end-labeled (^{32}P) antisense DNA oligonucleotides were used to detect miRNAs from total RNAs. 5′-end-labeled (^{32}P) antisense LNA oligonucleotides were used to detect miRNAs from AGO1 or AGO10 immunoprecipitation samples. The probe sequences are listed in Table S2.

Immunoprecipitation

FLAG-AGO1 immunoprecipitation was performed as described [20]. *ag-1 pAG::AG-GFP* and *zll-1 pZLL::YFP-ZLL* inflorescences were ground in liquid nitrogen and homogenized in an equal volume of extraction buffer (20 mM Tris HCl pH 7.5, 300 mM NaCl, 5 mM $MgCl_2$, 5 mM DTT, 1% (v/v) protease inhibitor cocktail (Roche, Cat# 11244800; 1 tablet was dissolved in 1 ml nuclease-free water)). The extracts were centrifuged for 10 min at 16,000 g three times to pellet any debris. The lysates were then precleared with protein-A agarose (Thermo Scientific, Cat# 20333) for 1 hr. Anti-GFP antibodies (Clontech, Cat# 632460) were added to the samples at a 1:200 dilution and the samples were incubated on a rotating shaker for 2 hrs. Protein-A agarose was added at a 1:50 ratio and incubation was continued for another 2 hrs. The immune complexes were washed four times with 1.5 ml of extraction buffer supplied with 0.5% NP-40 and two times with RISC (RNA-induced silencing complex) buffer (40 mM Hepes pH 7.4, 100 mM KOAc, 5 mM MgOAc, 4 mM DTT). Finally, the immune complexes were resuspended into 100 µl RISC buffer.

In vitro transcription and RNA cleavage assay

The *PHB* and *PHBm* cDNAs were amplified by PCR with primers *PHBprobeF* and *PHBprobeR* (see Table S2 for sequence information) from the wild type *PHB* and the miR165/166-resistant *PHB G202G* [30] templates, respectively. The PCR products were cloned into pGEM-T Easy (Promega, Cat#A1360) and selected clones were sequenced to ensure the absence of unwanted mutations. The clones were linearized with *Spe*I (NEB, Cat# R0133L) and the linearized DNA was gel purified. *In vitro* transcription and RNA cleavage assays were carried out as described [20]. *In vitro* transcription was performed by incubating 800 ng DNA in a 25 µl reaction with T7 RNA polymerase (Promega, Cat# P2077) and α-P^{32}-UTP at 37°C for 1.5 hrs. Labeled *PHB* and *PHBm* probes were gel purified and dissolved in 50 µl nuclease-free water. 3 µl probes were used in a 25 µl cleavage reaction mix containing 20 µl AGO1 or AGO10 immune complexes in RISC buffer, 1 µl 25 mM ATP and 1 µl RNase inhibitor (Fermentas, Cat# EO0381). The reaction mix was incubated at 37°C for 1.5 hrs. The RNAs were resolved in an 8 M Urea/5% polyacrylamide gel and detected with a Typhoon Phosphorimager.

Protein extraction and western blotting

To extract proteins from plants, 25 mg inflorescence material was ground in liquid nitrogen and homogenized with 150 µl 1XSDS loading buffer supplied with 0.5% (v/v) 2-mercaptoethanol and 1% (v/v) protease inhibitor cocktail mix. The extracts were boiled for 5 min, followed by centrifugation at 16,000 g at 4°C for 5 min. 15 µl supernatant was resolved in a 10% SDS-PAGE gel. To assay the AGO1 or AGO10 immunoprecipitation samples, 8 µl immune complexes were boiled with an equal volume of 2XSDS loading buffer with 1% (v/v) 2-mercaptoethanol and 2% protease inhibitor cocktail mix. The proteins were resolved in a 7.5% SDS-PAGE gel and a monoclonal anti-GFP antibody (Abcam, Cat# ab3277) was used for immunodetection.

Supporting Information

Figure S1 Diagrams of *AG*, *AGO10*, and *PHV* genes and multiple sequence alignments of *Arabidopsis* AGO proteins. (A) Diagrams of *AG*, *AGO10*, and *PHV*. In *ag-10*, the replacement of the guanine at nucleotide 3618 (position 1 being the "A" in the ACG start codon) by adenine causes an E-to-K substitution. *ago10-12* has a C-to-T transition at nucleotide 2991 (position 1 being the "A" in the ATG start codon), which results in an L-to-F substitution at amino acid 674 in the protein. *ago10-13* has a G-to-A transition at nucleotide 833, which introduces a premature stop codon in the second exon. *ago10-14* is a G-to-A mutation at nucleotide 3323 causing a D-to-N substitution. *phv-5d* contains a G-to-A transition at nucleotide 1410 (position 1 being the "A" in the ATG start codon), causing an G-to-D substitution. (B) Multiple sequence alignment of all *Arabidopsis* AGO proteins indicates that 674 L is conserved. (C) A diagram showing that the *phv-5d* mutation disrupts the binding site for miR165/166.
Found at: doi:10.1371/journal.pgen.1001358.s001 (12.36 MB TIF)

Figure S2 The accumulation of miRNAs, ta-siRNAs and their target mRNAs in *ago10* mutants. (A) Northern blotting to detect six miRNAs and three ta-siRNAs. The *ago10-13* mutation resulted in

slightly elevated levels of miR165/166 and slightly reduced levels of miR164. The other examined miRNAs were not obviously affected. The levels of siR255 (from *TAS1*), siR1511 (from *TAS2*), and 5D8(+) (from *TAS3*), were not affected by *ago10* mutations. The U6 blots served as loading controls for the overlying small RNA blots. The numbers below the small RNA blots indicate the relative abundance of the small RNAs. (B) Realtime RT-PCR to determine the levels of miRNA- and siRNA-targeted mRNAs. Most of the examined mRNAs were not significantly different between *ago10-13* and L*er* inflorescences. A small elevation was observed for *CUC1* mRNA targeted by miR164. Bars represent standard deviation of three technical replicates. Three biological replicates yielded similar results.
Found at: doi:10.1371/journal.pgen.1001358.s002 (4.92 MB TIF)

Figure S3 Floral phenotypes of various genotypes. (A) An *ago10-13* flower; *ago10-13* flowers resembled wild-type flowers except for the narrower petals. (B) Siliques from *ago10-13* plants. *ago10-13* siliques were shorter and wider than those of wild-type plants. (C) An SEM image of an *ago1-11* flower. (D) An *ago1-11 ago10-13*/+ inflorescence with obviously enlarged floral meristems (arrow). (E) A *wus-1* flower. (F, G) *hua1 hua2 ago10-12* and *clv3-1* exhibited synergistic effects in terms of floral determinacy. (F) A *hua1 hua2 ago10-12 clv3-1* flower with an enlarged gynoecium. (G) A *hua1 hua2 ago10-12 clv3-1* silique with a massive amount of internal stigma tissue bursting out of the primary gynoecium. (H) Third whorl organs in *hua1 hua2 ago10-12* flowers. Some had petaloid features (the two on the left) while others resembled stamens. (I-L) SEM images of anthers and anther epidermal cells in *hua1 hua2 ago10-12* (I and J) and *hua1 hua2 ago10-12 ap2-2* (K and L). (M) Siliques of *ag-10 ap2-2* plants. (N) Siliques of *ag-10 ago10-13* plants. Note the elongated gynophore (arrow). (O) Siliques of *ag-10 ago10-13 ap2-2* plants. (P) Quantification of gynophore length in the two genotypes. (Q) Siliques of *phb-1d*/+ plants. (R) *ag-10 ago10-13*/+ *phb-1d*/+ siliques showing gynoecia enlargement and the presence of ectopic organs (indicated by the arrows). (S) Bulged siliques and ectopic floral organs, indicated by the arrows, were found in *ag-10 phv-5d*/+ plants. (T) An *ag-10* amiR165/166 plant showing SAM defects reminiscent of *ago10* mutants. Scale bar, 500 μm in (C), 300 μm in (I), (K), 50 μm in (J), (L), and 1 mm in the rest of the panels.
Found at: doi:10.1371/journal.pgen.1001358.s003 (15.43 MB TIF)

Figure S4 AGO10 does not bind miR390. Northern blots for miR166 and miR390 were performed for total RNAs from wild type (L*er*; the three lanes on the right) and immunoprecipitated samples (the first two lanes from the left) using anti-GFP antibodies from L*er* (a negative control) and the *YFP-ZLL* transgenic line. YFP-ZLL was associated with miR166 but not miR390 *in vivo*.
Found at: doi:10.1371/journal.pgen.1001358.s004 (1.75 MB TIF)

Figure S5 The expression of *ZPR3* in wild type (L*er*) and *ago10-13* as determined by realtime RT-PCR.
Found at: doi:10.1371/journal.pgen.1001358.s005 (2.62 MB TIF)

Figure S6 A diagram of amiR165/166. A modified, partial pri-miR168 is highlighted in black. The amiR165 and amiR166 sequences (in green) were introduced into the pri-miR168 backbone through two rounds of PCR cloning using the *Swa*I and *Pme*I sites, respectively. The whole structure was inserted between a 2X35S promoter and a 35S terminator through the restriction sites *Hin*dIII and *Eco*RI.
Found at: doi:10.1371/journal.pgen.1001358.s006 (0.11 MB JPG)

Table S1 Floral organ counts in various genotypes.
Found at: doi:10.1371/journal.pgen.1001358.s007 (0.06 MB PDF)

Table S2 Sequences of oligonucleotides used in this study.
Found at: doi:10.1371/journal.pgen.1001358.s008 (0.11 MB DOC)

Acknowledgments

We thank Kathy Barton, David Baulcombe, Jennifer Fletcher, Thomas Laux, Allison Mallory, Elliot Meyerowitz, and Patricia Springer for sharing reagents and strains. We thank Kiet Nguyen for technical assistance and Yuanyuan Zhao for comments on the manuscript.

Author Contributions

Conceived and designed the experiments: X Chen, L Ji, X Liu, W Wang, RE Yumul, X Cui, X Cao, G Tang. Performed the experiments: X Chen, L Ji, X Liu, J Yan, W Wang, RE Yumul, YJ Kim, TT Dinh, J Liu, X Cui, B Zheng, M Agarwal, C Liu. Analyzed the data: X Chen, L Ji, X Liu, W Wang, RE Yumul, YJ Kim, TT Dinh, J Liu, B Zheng, M Agarwal, C Liu. Contributed reagents/materials/analysis tools: J Yan, G Tang. Wrote the paper: X Chen, L Ji, RE Yumul.

References

1. Sablowski R (2007) Flowering and determinacy in *Arabidopsis*. J Exp Bot 58: 899–907.
2. Laux T, Mayer KF, Berger J, Jurgens G (1996) The *WUSCHEL* gene is required for shoot and floral meristem integrity in *Arabidopsis*. Development 122: 87–96.
3. Smyth DR, Bowman JL, Meyerowitz EM (1990) Early flower development in *Arabidopsis*. Plant Cell 2: 755–767.
4. Schoof H, Lenhard M, Haecker A, Mayer KF, Jurgens G, et al. (2000) The stem cell population of *Arabidopsis* shoot meristems in maintained by a regulatory loop between the *CLAVATA* and *WUSCHEL* genes. Cell 100: 635–644.
5. Irish VF (2010) The flowering of *Arabidopsis* flower development. Plant J 61: 1014–1028.
6. Lenhard M, Bohnert A, Jurgens G, Laux T (2001) Termination of stem cell maintenance in *Arabidopsis* floral meristems by interactions between *WUSCHEL* and *AGAMOUS*. Cell 105: 805–814.
7. Lohmann JU, Hong RL, Hobe M, Busch MA, Parcy F, et al. (2001) A molecular link between stem cell regulation and floral patterning in *Arabidopsis*. Cell 105: 793–803.
8. Bowman JL, Smyth DR, Meyerowitz EM (1989) Genes directing flower development in *Arabidopsis*. Plant Cell 1: 37–52.
9. Jofuku KD, den Boer BG, Van Montagu M, Okamuro JK (1994) Control of *Arabidopsis* flower and seed development by the homeotic gene *APETALA2*. Plant Cell 6: 1211–1225.
10. Aukerman MJ, Sakai H (2003) Regulation of flowering time and floral organ identity by a microRNA and its *APETALA2*-like target genes. Plant Cell 15: 2730–2741.
11. Chen X (2004) A microRNA as a translational repressor of *APETALA2* in *Arabidopsis* flower development. Science 303: 2022–2025.
12. Zhao L, Kim Y, Dinh TT, Chen X (2007) miR172 regulates stem cell fate and defines the inner boundary of APETALA3 and PISTILLATA expression domain in Arabidopsis floral meristems. Plant J 51: 840–849.
13. Drews GN, Bowman JL, Meyerowitz EM (1991) Negative regulation of the *Arabidopsis* homeotic gene *AGAMOUS* by *APETALA2* product. Cell 65: 991–1002.
14. Chen X (2009) Small RNAs and their roles in plant development. Annu Rev Cell Dev Biol 25: 21–44.
15. Hock J, Meister G (2008) The Argonaute protein family. Genome Biol 9: 210.
16. Havecker ER, Wallbridge LM, Hardcastle TJ, Bush MS, Kelly KA, et al. (2010) The *Arabidopsis* RNA-directed DNA methylation argonautes functionally diverge based on their expression and interaction with target loci. Plant Cell 22: 321–334.
17. Mi S, Cai T, Hu Y, Chen Y, Hodges E, et al. (2008) Sorting of small RNAs into *Arabidopsis* argonaute complexes is directed by the 5′ terminal nucleotide. Cell 133: 116–127.
18. Montgomery TA, Howell MD, Cuperus JT, Li D, Hansen JE, et al. (2008) Specificity of ARGONAUTE7-miR390 interaction and dual functionality in *TAS3* trans-acting siRNA formation. Cell 133: 128–141.
19. Zheng X, Zhu J, Kapoor A, Zhu JK (2007) Role of Arabidopsis AGO6 in siRNA accumulation, DNA methylation and transcriptional gene silencing. Embo J 26: 1691–1701.

20. Baumberger N, Baulcombe DC (2005) *Arabidopsis* ARGONAUTE1 is an RNA Slicer that selectively recruits microRNAs and short interfering RNAs. Proc Natl Acad Sci U S A 102: 11928–11933.
21. Vaucheret H (2008) Plant ARGONAUTES. Trends Plant Sci 13: 350–358.
22. Bohmert K, Camus I, Bellini C, Bouchez D, Caboche M, et al. (1998) *AGO1* defines a novel locus of *Arabidopsis* controlling leaf development. Embo J 17: 170–180.
23. Lynn K, Fernandez A, Aida M, Sedbrook J, Tasaka M, et al. (1999) The *PINHEAD/ZWILLE* gene acts pleiotropically in *Arabidopsis* development and has overlapping functions with the *ARGONAUTE1* gene. Development 126: 469–481.
24. Moussian B, Schoof H, Haecker A, Jurgens G, Laux T (1998) Role of the *ZWILLE* gene in the regulation of central shoot meristem cell fate during *Arabidopsis* embryogenesis. Embo J 17: 1799–1809.
25. McConnell JR, Barton MK (1995) Effect of mutations in the *PINHEAD* gene of *Arabidopsis* on the formation of shoot apical meristems. Dev Genet 16: 358–366.
26. Brodersen P, Sakvarelidze-Achard L, Bruun-Rasmussen M, Dunoyer P, Yamamoto YY, et al. (2008) Widespread translational inhibition by plant miRNAs and siRNAs. Science 320: 1185–1190.
27. Mallory AC, Hinze A, Tucker MR, Bouche N, Gasciolli V, et al. (2009) Redundant and specific roles of the ARGONAUTE proteins AGO1 and ZLL in development and small RNA-directed gene silencing. PLoS Genet 5: e1000646. doi:10.1371/journal.pgen.1000646.
28. Cheng Y, Kato N, Wang W, Li J, Chen X (2003) Two RNA binding proteins, HEN4 and HUA1, act in the processing of *AGAMOUS* pre-mRNA in *Arabidopsis thaliana*. Dev Cell 4: 53–66.
29. Emery JF, Floyd SK, Alvarez J, Eshed Y, Hawker NP, et al. (2003) Radial patterning of *Arabidopsis* shoots by class III HD-ZIP and *KANADI* genes. Curr Biol 13: 1768–1774.
30. Mallory AC, Reinhart BJ, Jones-Rhoades MW, Tang G, Zamore PD, et al. (2004) MicroRNA control of *PHABULOSA* in leaf development: importance of pairing to the microRNA 5′ region. Embo J 23: 3356–3364.
31. Chen X, Meyerowitz EM (1999) *HUA1* and *HUA2* are two members of the floral homeotic *AGAMOUS* pathway. Mol Cell 3: 349–360.
32. Chen X, Liu J, Cheng Y, Jia D (2002) *HEN1* functions pleiotropically in *Arabidopsis* development and acts in C function in the flower. Development 129: 1085–1094.
33. Li J, Chen X (2003) PAUSED, a putative exportin-t, acts pleiotropically in *Arabidopsis* development but is dispensable for viability. Plant Physiol 132: 1913–1924.
34. Wang W, Chen X (2004) HUA ENHANCER3 reveals a role for a cyclin-dependent protein kinase in the specification of floral organ identity in Arabidopsis. Development 131: 3147–3156.
35. Western TL, Cheng Y, Liu J, Chen X (2002) HUA ENHANCER2, a putative DExH-box RNA helicase, maintains homeotic B and C gene expression in Arabidopsis. Development 129: 1569–1581.
36. Tucker MR, Hinze A, Tucker EJ, Takada S, Jurgens G, et al. (2008) Vascular signalling mediated by *ZWILLE* potentiates *WUSCHEL* function during shoot meristem stem cell development in the *Arabidopsis* embryo. Development 135: 2839–2843.
37. Mayer KF, Schoof H, Haecker A, Lenhard M, Jurgens G, et al. (1998) Role of WUSCHEL in regulating stem cell fate in the Arabidopsis shoot meristem. Cell 95: 805–815.
38. Clark SE, Running MP, Meyerowitz EM (1995) *CLAVATA3* is a specific regulator of shoot and floral meristem development affecting the same processes as *CLAVATA1*. Development 121: 2057–2067.
39. Kidner CA, Martienssen RA (2005) The role of *ARGONAUTE1* (*AGO1*) in meristem formation and identity. Dev Biol 280: 504–517.
40. Park W, Li J, Song R, Messing J, Chen X (2002) CARPEL FACTORY, a Dicer homolog, and HEN1, a novel protein, act in microRNA metabolism in *Arabidopsis thaliana*. Curr Biol 12: 1484–1495.
41. Baker CC, Sieber P, Wellmer F, Meyerowitz EM (2005) The *early extra petals1* mutant uncovers a role for microRNA miR164c in regulating petal number in *Arabidopsis*. Curr Biol 15: 303–315.
42. McConnell JR, Barton MK (1998) Leaf polarity and meristem formation in *Arabidopsis*. Development 125: 2935–2942.
43. Liu Q, Yao X, Pi L, Wang H, Cui X, et al. (2008) The *ARGONAUTE10* gene modulates shoot apical meristem maintenance and leaf polarity establishment by repressing miR165/166 in *Arabidopsis*. Plant J.
44. Wenkel S, Emery J, Hou BH, Evans MM, Barton MK (2007) A feedback regulatory module formed by LITTLE ZIPPER and HD-ZIPIII genes. Plant Cell 19: 3379–3390.
45. Qi Y, He X, Wang XJ, Kohany O, Jurka J, et al. (2006) Distinct catalytic and non-catalytic roles of ARGONAUTE4 in RNA-directed DNA methylation. Nature 443: 1008–1012.
46. Vaucheret H, Vazquez F, Crete P, Bartel DP (2004) The action of ARGONAUTE1 in the miRNA pathway and its regulation by the miRNA pathway are crucial for plant development. Genes Dev 18: 1187–1197.
47. Sun B, Xu Y, Ng KH, Ito T (2009) A timing mechanism for stem cell maintenance and differentiation in the *Arabidopsis* floral meristem. Genes Dev 23: 1791–1804.
48. Prigge MJ, Otsuga D, Alonso JM, Ecker JR, Drews GN, et al. (2005) Class III homeodomain-leucine zipper gene family members have overlapping, antagonistic, and distinct roles in *Arabidopsis* development. Plant Cell 17: 61–76.
49. Zhou GK, Kubo M, Zhong R, Demura T, Ye ZH (2007) Overexpression of miR165 affects apical meristem formation, organ polarity establishment and vascular development in Arabidopsis. Plant Cell Physiol 48: 391–404.
50. Bowman JL, Smyth DR, Meyerowitz EM (1991) Genetic interactions among floral homeotic genes of *Arabidopsis*. Development 112: 1–20.
51. Pall GS, Codony-Servat C, Byrne J, Ritchie L, Hamilton A (2007) Carbodiimide-mediated cross-linking of RNA to nylon membranes improves the detection of siRNA, miRNA and piRNA by northern blot. Nucleic Acids Res 35: e60.